

Fourier-Transformed Alternating Current Voltammetry (FTacV) for Analysis of Electrocatalysts

Rifael Z. Snitkoff-Sol, Alan M. Bond, and Lior Elbaz*

Cite This: *ACS Catal.* 2024, 14, 7576–7588

Read Online

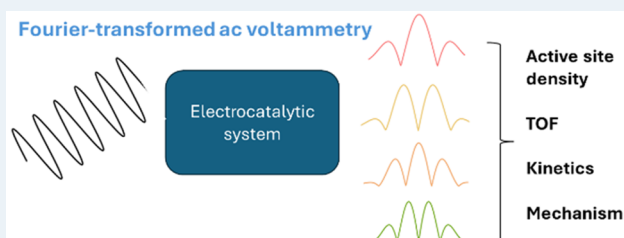
ACCESS |

Metrics & More

Article Recommendations

ABSTRACT: Electrocatalysts play a critical role in energy technologies, but the development of active, efficient, and durable catalysts is impeded by the lack of methodologies to deconvolute the complex interplay between various aspects influencing the activity of the catalysts, e.g., the number of active sites, turnover frequency, and the reaction pathways. Fourier-transformed alternating current voltammetry (FTacV) is an emerging tool for the analysis of electroactive species and has been successfully applied to a variety of reactions such as the oxygen reduction reaction, oxygen evolution reaction, carbon dioxide reduction reaction, hydrogen evolution reaction, and hydrogen oxidation reaction. The harmonics generated from FTacV measurements neatly detect underlying processes not visible by other, more commonly employed techniques for analysis of electrocatalysts, such as the rotating disc electrode and dc voltammetry. The harmonic components enable separating overlapping processes based on differences in kinetics or linearity of response. This paper presents a review of FTacV applied for the analysis of electrocatalysts. It highlights the importance of determining the electrochemically active site density (EASD) to decipher the intrinsic activity of a catalyst and discusses the use of FTacV in dynamic determination of the EASD over the course of a catalyst's working life, as well as the use of FTacV to understand intricate catalytic processes.

KEYWORDS: electrocatalysis, active-site density, Fourier-transformed alternating current voltammetry, hydrogen evolution reaction, oxygen reduction reaction, carbon dioxide reduction



1. INTRODUCTION

Electrocatalysts play a major role in sustainable energy technologies, which are required to fight climate change and reduce the environmental impact of fossil fuel based energy production.¹ Technologies such as fuel cells,² electrolyzers,³ and water purification systems⁴ utilize electrocatalysis to facilitate the necessary electrochemical reactions.^{5–8}

Electrocatalysts reduce the activation energy of electrochemical reactions by interacting with the reacting species on an active site. For example, in multistep reactions, adsorption of the reactant and the reaction intermediates on the active sites changes the reaction mechanism without influencing the thermodynamics of the overall reaction, i.e., changing only the rate of the reactions.⁹ The adsorption energies of different intermediates in a multistep reaction on an active site influence the activity of a catalyst and are a fundamental aspects of heterogeneous electrocatalysis.⁹

The use of volcano plots, where the activity is plotted against the adsorption energy of a single reaction intermediate,¹⁰ highlights the importance of quantifying the adsorption energies.^{1,11} These energies govern the thermodynamics of each elementary step, and their quantification enables the construction of a free energy diagram at different electrode potentials, leading to the possibility of uncovering the identity

of the potential determining step for the proposed reaction scheme.^{12–15}

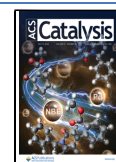
Such free energy diagrams are oblivious to the activation energies at equilibrium of the elementary steps, and thus these parameters should also be found in order to gain a comprehensive understanding of the activity of a catalyst.^{16–23} The intrinsic activity of catalysts is quantified by the number of reacting molecules an active site transforms per unit of time, termed the turnover frequency (TOF), which is a function of the thermodynamics (governed by the adsorption energies of the intermediates), as well as the kinetics of the elementary steps (governed by the activation energies). To determine the TOF, the number of available active sites, the electrochemically active site density (EASD) must be quantified. When multiple active sites with different TOFs are present in a single catalyst, the quantification of the number of sites, as well as the TOF of each species of catalysts should be carefully

Received: March 12, 2024

Revised: April 18, 2024

Accepted: April 19, 2024

Published: May 1, 2024



determined.²⁴ The resulting TOF is an average of the TOF of the different reacting active sites, each having a different surface concentration and a different TOF, as shown in eq 1:

$$\text{TOF} = \sum_j \theta_j \text{TOF}_j \quad (1)$$

with θ_j being the fraction of sites of species j that are exposed to the reactant. Thus, the ability to measure the EASD is crucial to decipher the intrinsic activity of a catalyst and its species if possible. Additionally, the dynamic determination of the EASD of a catalyst over the course of the catalyst's working life is needed to determine degradation mechanisms and develop more durable catalysts.

The use of electroanalytical methods for the analysis of the activity of electrocatalysts has regained interest in the past years. The lack of methodologies to deconvolute the intrinsic activity of the active-sites (i.e., TOF) and the number of sites impeded the design and development of novel, efficient, and durable catalysts. In contrast to the ubiquitous cyclic voltammetry (CV) and rotating disc electrode (RDE) measurements that are widely employed for the analysis of electrocatalysts, Fourier-transformed alternating current voltammetry (FTacV) emerged in recent years as a powerful tool for analysis of electroactive species.

The ability to exploit the high kinetic sensitivity and selectivity provided by analysis of the higher harmonic components generated in FTacV measurements was recognized over 20 years ago by the Monash Electrochemistry Group.²⁵ Earlier versions were predominantly confined to small amplitudes (≤ 10 mV) and examination of the fundamental and second harmonics.²⁶ Use of large sinewave amplitudes, up to 300 mV, to study electrochemical reactions is advantageous as multiple harmonics are generated in a single experiment. The enhanced kinetic sensitivity of the higher-order harmonic components to electrode kinetics allows discrimination of fast reactions at or near the reversible limit (generating multiple harmonics) from those at or near the irreversible limit (generating few harmonics) and also of background charging current which is absent or minimal in third and higher-order harmonics, and thus have been applied successfully to analyze mechanisms of electrochemical reactions in diverse systems such as aqueous media,^{27–32} organic solvents,^{33–37} molten metals and salts,^{38–41} ionic liquids,^{33,42–44} and fuel cells.^{45,46} FTacV is especially suited for the analysis of many energy-related electrocatalysts and has been applied to a variety of reactions such as the oxygen reduction reaction (ORR),⁴⁵ oxygen evolution reaction (OER),^{47–49} carbon dioxide reduction reaction (CO₂RR),^{32,50,51} hydrogen evolution reaction (HER),⁵² and hydrogen oxidation reaction (HOR),³¹ as well as other catalytic reactions such as hydrazine oxidation,⁵³ and nitrite/nitrate reduction.⁴⁹

The sensitivity of the FTacV technique to the kinetics of electrochemical reactions enables retrieving invaluable experimental data on the catalytic active site as well as on the mechanism of the catalytic reaction. The elucidation of mechanisms and quantification of reaction parameters from FTacV measurements are facilitated by the in-house developed, free-of-charge, numerical simulator, the Monash Electrochemistry Simulator package (MECSim).^{54,55} It is especially noteworthy, that by using BIOMECH, a Bayesian inference and data optimization application developed for

MECSim by Gundry et al., statistical analysis of the extracted parameters' values becomes straightforward.^{56–58}

Herein, we review the use of large amplitude FTacV for the analysis of heterogeneous electrocatalysts and show the wide range of scientific questions to which it can be applied. The first section is written to familiarize the readers with the harmonics generated from FTacV experiments and show how they are influenced by the cell and input parameters. Next, the use of FTacV for the analysis of heterogeneous electrocatalysts will be overviewed. Special focus will be given to investigations where FTacV was applied to uncover masked redox transitions, determine the EASD of an electrocatalyst, and extract kinetic and thermodynamic parameters of charge-transfer reactions.

2. FOURIER-TRANSFORMED ALTERNATING CURRENT VOLTAMMETRY: A SHORT TUTORIAL

In the most common form of FTacV a sinewave is superimposed on a potential ramp as illustrated in Figure 1

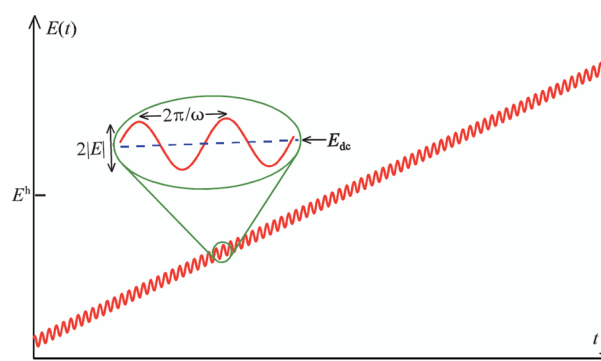


Figure 1. Illustration of the applied potential in an FTacV measurement versus time. A sinewave potential with an amplitude of $|E|$ and a frequency of ω is superimposed on a potential ramp $E_{dc} = E_i + vt$ (eq 2). Reprinted by permission of John Wiley & Sons – Books from ref 8. Permission conveyed through Copyright Clearance Center, Inc.

following eq 2, where E is the applied potential and E_i is the initial potential. The scan rate, v , should be low so the dc and ac time scales do not overlap and is usually given in $[V s^{-1}]$, t is the time given in $[s]$, $|E|$ is the amplitude given in $[V]$, and ω is the frequency given in $[Rad s^{-1}]$. The amplitude ($|E|$ in eq 2, half the peak-to-peak value) of the sinewave needs to be large enough to induce substantial nonlinearities in the currents that arise from charge-transfer reactions as illustrated in Figure 2 where the effect of the applied amplitude on the current is depicted for the case of a faradaic charge-transfer reaction described by the Butler–Volmer phenomenological charge-transfer model.⁵⁹

$$E(t) = E_i + vt + |E|\sin(\omega t) \quad (2)$$

Figure 3 illustrates the procedure for extracting the harmonic components from the total current generated in FTacV measurements, for the case of a charge-transfer reaction followed by a chemical step, as an example of an electrocatalytic reaction. The resulting current undergoes filtering to discriminate between the current arising from charge-transfer reactions and the non-faradaic background currents. This is achieved by converting the experimental raw data, i.e., the total current (Figure 3a) to the frequency domain via a Fourier transform (FT) algorithm where individual harmonic

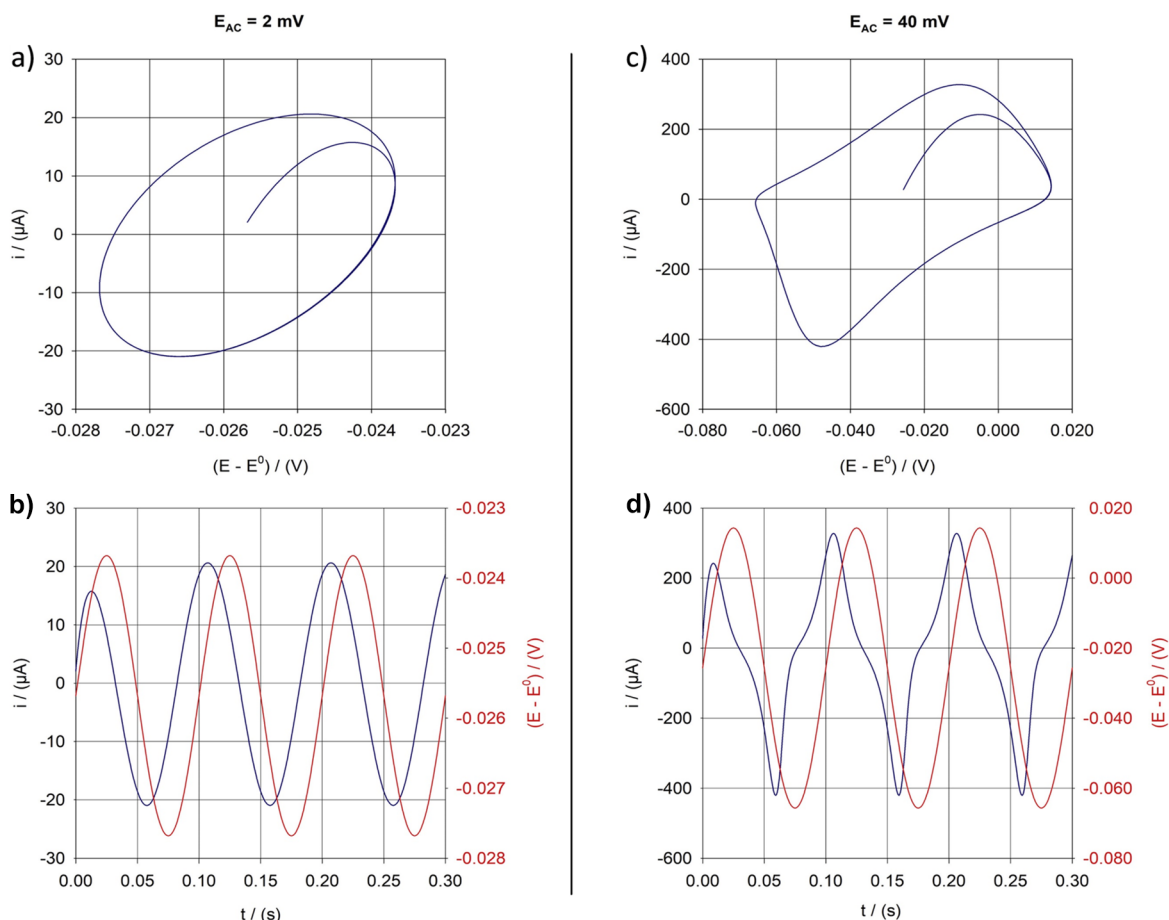


Figure 2. Illustration of the effect of the amplitude of the sinewave on the generated current. **a)** Current (i) versus ac potential ($E - E^0$) for the case of a low amplitude potential sinewave ($|E| = 0.002$ V). In this case the response is linear with respect to the potential and the generated current is a single sinewave at the applied frequency as depicted in **b)**, where the applied potential (red) and generated current (blue) are plotted versus time. **c)** Current versus ac potential for the case of a large amplitude ($|E| = 0.040$ V). In this case the response is nonlinear with respect to the potential and the generated current no longer shows a response resembling a single sinewave as depicted in **d)**, where the applied potential (red) and generated current (blue) are plotted versus time. The generated current can be represented by a sum of sinewaves each with a frequency at a multiple of the fundamental (applied) frequency, which are the harmonic components utilized in the FTacV data analysis. The simulation is for the case of a reversible surface-confined electron-transfer process ($O^* + e^- \rightleftharpoons R^*$) with a reversible potential E^0 . For more details on the model and parameters used and other missing features please refer to ref 59. Parameters: frequency $f = 10$ Hz, scan rate, $\nu = 0$ s $^{-1}$. Reprinted from ref 59 with permission from Elsevier.

components are distinguishable. Each harmonic is filtered using a band-pass filter which nulls the contribution of other harmonic components. The data is then converted back to the time domain by applying an inverse FT algorithm (Figure 3b). 2^N data points, where N is an integer, in the range of 14–20, are used to utilize the fast FT algorithm.⁶⁰

It is illuminating to consider in more detail the response of the example given above and depicted in Figure 3 for an electrocatalytic reaction in an FTacV measurement. The reaction is as follows; in the first step, a faradaic charge-transfer step occurs,



where “*” indicates a surface-confined species, O^* and R^* are the oxidized and reduced states of the surface-confined species, respectively. We omit for convenience the coupled ion-transfer step that balances the charge.^{61,62} Following the charge-transfer step is a chemical step:



where A and B are the reactant and product of the chemical step found in solution, respectively. Thus, species A in solution reacts with the reduced state of the surface-confined species (R^*), forming the oxidized state (O^*) which is further reduced back to R^* by a charge-transfer step (eq 3), continuing the catalytic cycle. The faradaic current due to the electron-transfer step (eq 3) will be modified by the catalytic reaction described by eq 4. The response of these reactions to a large-amplitude potential sinewave superimposed on a potential ramp was investigated by Zhang and Bond. They presented analytical solutions for the aperiodic dc and higher harmonic components for the case where the charge-transfer step (eq 3) is fast and follows the Nernst equation (i.e., thermodynamically reversible).⁶³ Their results showed that the harmonic components are modified in a manner related to the order of the harmonic and the rate constant of eq 4. They showed that when the rate constant of eq 4 is very small, the faradaic current due to the charge-transfer reaction (eq 3) is fully resolvable in the third and higher order harmonic components and is independent of the catalytic current. For catalytic reactions showing faster kinetics, the magnitude of the current

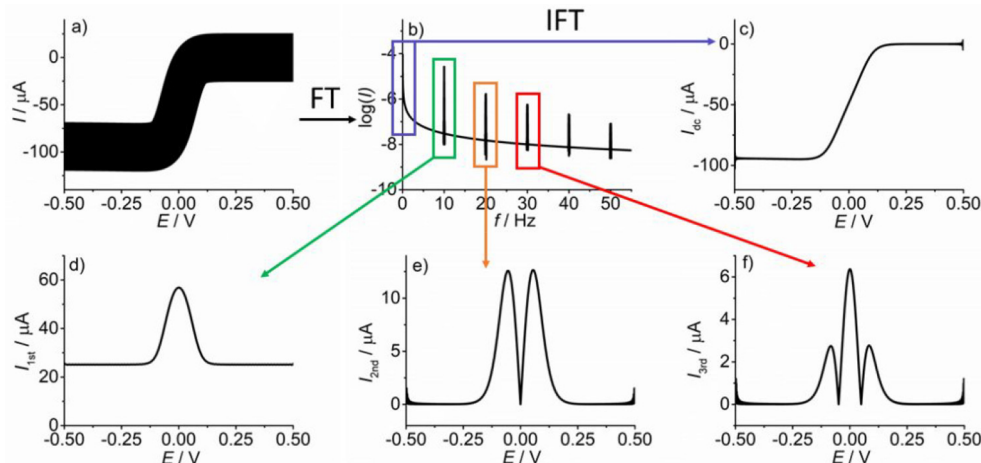


Figure 3. Schematics of the extraction of the harmonic current from the total current measured during an FTacV measurement of a reversible surface-confined electron-transfer process ($O^* + e^- \rightleftharpoons R^*$) followed by a catalytic reaction ($R^* + A \rightleftharpoons O^* + B$), where “*” indicates a surface-confined catalytic site, O^* and R^* are the oxidized and reduced states of the surface-confined species, respectively. A and B are the reactant and product of the chemical step, respectively. **a)** Raw data from FTacV measurements. i , current; E , voltage. **b)** Analysis of the data using the Fourier transform (FT) algorithm, which converts the current from the time domain to the frequency domain where it can be plotted as a power spectrum. Each band in the power spectrum is a harmonic of the fundamental frequency at an integer multiple of the latter’s frequency. Each harmonic is selected using a window filter (rectangles in **b**) while nulling the remaining data. **c)** Filtered dc current, **d)** fundamental, **e)** second, and **f)** third harmonics after transformation back to the time domain via the inverse FT algorithm. The harmonic current is plotted versus the DC potential. Simulated using DigiElch. Parameters: catalyst surface coverage $\Gamma_{O^*} = 1 \times 10^{-11} \text{ mol cm}^{-2}$, reversible potential $E^0 = 0.00 \text{ V}$, electrode area $A = 0.10 \text{ cm}^2$, rate constant for catalytic reaction $k_{cat} = 1000 \text{ s}^{-1} \text{ M}^{-1}$, double-layer capacitance $C_{dl} = 5 \times 10^{-6} \text{ farad cm}^{-2}$, frequency $f = 10 \text{ Hz}$, amplitude $|E| = 0.080 \text{ V}$, scan rate $\nu = 0.010 \text{ V s}^{-1}$, and temperature $T = 298 \text{ K}$. Reprinted with permission from ref 60. Copyright American Chemical Society.

Table 1. Summary of Free of Charge Resources Available for Analysis of FTacV Experiments and Simulations

Resource Name	Resource Description	Available to download at
Monash ElectroChemistry Simulator (MECSim)	Digital simulation software package that can model a large variety of electrochemical systems and mechanisms	http://www.garethkennedy.net/MECSim.html
Bayesian Inference and Optimization for the Monash ElectroChemical Simulator (BIOMECH)	A platform for automatic parametrization and Bayesian inference of electrochemical experiments simulated using the MECSim software package	https://github.com/lukegun/BIOEMEC
Harmonic view (HRview)	Software for analysis of FTacV experiments and simulations. Interfaces with MECSim.	https://github.com/friedmanariel/HRview?tab=readme-ov-file
FTacV Surface Confined Simulation (FTacV_SC_Simulation)	Software developed for building intuition towards the harmonic components generated in FTacV experiments	https://github.com/Snitkoff-Sol/FTacV_SC_Simulation

in the harmonic components increased, with the effect decreasing with the harmonic order. In contrast, if the charge-transfer step (eq 3) is very slow, then the current in third and higher harmonics will be negligible, independently of the catalytic current.

In summary, if a process that has fast electrode kinetics overlaps with one having slow electrode kinetics or which behaves irreversibly because of a slow electron-transfer step coupled to a fast chemical step, the higher order harmonic components will essentially only contain information relevant to the fast process. Since background current based on an ideal double layer capacitance model is predicted to be devoid of second and higher order harmonics, the use of the higher order harmonics accessible in FTacV is often very attractive to discriminate against overlapping irreversible processes and/or background current in studies of electrocatalytic processes that commonly have a reversible or close to reversible underlying electron transfer reaction as in eq 3.

Next, the influence of the cell and experimental parameters, i.e., uncompensated resistance (R_u), double layer capacitance (C_{dl}), amplitude ($|E|$), and frequency (f), on the harmonic components is qualitatively analyzed below. Note that the analysis is restricted to a charge-transfer reaction described by

eq 3 without a coupled chemical step. It is vital for any practitioner wishing to use the technique to simulate a large range of experiments with a diverse set of parameters to gain intuition toward the output of the FTacV measurement. This can be accomplished by experimenting with a program designed in this work that was specifically developed for newcomers.⁶⁴ For a broader range of possible systems to simulate please refer to the program recently published by Friedman et al.^{65,66} which is an easy to use platform for data analysis as well as simulation using the MECSim software package. Table 1 summarizes available free of charge resources for the data analysis of FTacV experiments.

2.1. Uncompensated Resistance. The uncompensated resistance, arising from the resistance between the working and reference electrodes, reduces the magnitude of the effective sinewave amplitude (eq 4).⁶⁷ This can distort the shape of the higher harmonics and reduce the absolute magnitude of the harmonic currents, as well as the relative current magnitude between the harmonic components.^{68,69} Slow electron transfer kinetics has the same effects on the harmonic currents,³⁷ making the independent determination of the uncompensated resistance highly desirable.⁷⁰

2.2. Double Layer Capacitance. In cases of high surface-area electrodes, large capacitive currents are generated from the electrode surface charging. The capacitive current adds to the total current and increases the potential drop due to the uncompensated resistance according to eqs 5 and 6, indirectly influencing the magnitude and shape of the higher harmonics as explained in section 2.1.

$$I_{\text{tot}}(t) = I_f(t) + I_c(t) \quad (5)$$

$$E_{\text{eff}}(t) = E(t) - I_{\text{tot}}(t)R_u \quad (6)$$

In eqs 5 and 6, $I_{\text{tot}}(t)$ is the total current in [A], $I_f(t)$ and $I_c(t)$ are the faradaic and capacitive currents, respectively, both in [A]. The applied potential, $E(t)$, is described in eq 2, $E_{\text{eff}}(t)$, is the effective potential applied to the electrode, both in [V]. R_u is the uncompensated resistance in [Ohm]. Additionally, the capacitive current may vary over the scanned potential range,⁴² generating currents in harmonic components and interfering with the data analysis. This effect is usually limited up to the third harmonic, leaving the fourth and higher harmonic components free of capacitive currents. The effect of nonlinear capacitance is circumvented by empirically fitting the fundamental harmonic component to a parametric function and incorporating the outcome when simulating the experiment.⁷¹

2.3. Sinewave Amplitude. The magnitude of the harmonics is especially influenced by the amplitude of the applied sinewave. Figure 2 shows the ac current generated using small (Figure 2a and b) and large (Figure 2c and d) sinewave amplitudes. The former is clearly sinusoidal while the latter is more complicated. When performing a FT on a small amplitude ac current, only a single harmonic component is needed to obtain this signal (i.e., the fundamental harmonic), while in the case of a large amplitude, due to the nonlinearity, multiple sinewaves are needed to reconstruct the signal in the frequency domain, giving rise to the sought-after harmonic components. By increasing the amplitude of the sinewave, higher harmonic components can be generated and larger harmonic currents are obtained, signal-to-noise ratio.³⁰ However, the capacitive current also increases with the amplitude,³⁰ and the potential drop increases due to the increase in the total current, which, as mentioned above will in turn, lower the harmonic currents and deform their shape. Thus, the amplitude should be high enough such that the harmonic components are formed and can be clearly analyzed but should be as low as possible to reduce uncompensated resistance effects. Typically, the amplitude is in the range of 80–250 mV. It is noteworthy that in the case where multiple surface-confined species are present with close reversible redox potentials, increasing the amplitude reduces the resolution as the generated currents overlap.^{72,73}

2.4. Sinewave Frequency. The probing time scale of the measurement is determined by the frequency of the applied sinewave. For a large amplitude sinewave, the sensitivity to the kinetics of an electrochemical reaction is influenced by the magnitude of the frequency. The higher the frequency, the higher the kinetics that can be determined.⁶⁹ For example, in the case of a surface-confined single charge-transfer process with a relatively slow charge-transfer rate, low frequency measurements would suffice for the unambiguous determination of the rate constant. In contrast, in the case that the reaction rate is fast, high frequencies are needed.⁶⁹ Hence, if

the frequency will be too low, only a lower bound for the value of the rate constant can be determined.^{29,74}

An additional implication of increasing the frequency is the rise of nonidealities. Kinetic dispersion, where the rate of the charge-transfer reaction diverges between surface-confined species,⁷⁵ is of paramount importance and arises often in surface-confined voltammetry. For example, in the case of heterogeneous electrocatalysis where the reactant is in solution and the catalyst is confined to the surface, increasing the sinewave frequency may cause a decrease in the overlap between diffusion layers of reactants in solution,⁷⁶ which will enhance the effect of kinetic dispersion. This point is important for analysis of electrocatalysis as the kinetic parameters extracted in the opposite case, i.e., low frequency measurements, are always averaged out over the whole surface as the diffusion layers of the reacting species overlap. In cases where no catalysis occurs, at sufficiently low frequencies such that the faradaic reaction is near the reversible limit, the number of active-sites can be determined as well as other cell parameters.⁷⁷ The harmonic current is proportional to the number of accessible electroactive species, but it cannot be determined without simulations from measurements at frequencies where the kinetics and the uncompensated resistance have a large impact on the magnitude of the current in the higher harmonics.

Beyond the ideal case of the surface-confined species considered above, it is noteworthy to mention that there are several interesting phenomena that influence the current's magnitude and shape of the harmonic components. Surface-confined species may interact and show a non-Langmuirian adsorption isotherm. This will cause changes in the harmonic current similar to the broadening/narrowing of the redox reaction peaks in dcV. Another interesting phenomenon occurs when similar active sites reside in different environments on the surface, affecting the kinetics and the thermodynamics of the reaction. The effect of kinetic and thermodynamic dispersion on the harmonic components has been thoroughly investigated and experimentally determined for electroactive surface-confined enzymes.^{78,79} It was found that the relative current magnitude between the harmonic components changed considerably, with the effect increasing with harmonic order.⁷⁵ This effect is important for electrocatalysis, as both of the above phenomena impact the catalysis, as the elementary steps are related via scaling relations between various adsorbed species,¹¹ and thus measuring and accounting for these effects is crucial for fundamental understanding of the catalysis.

3. ANALYSIS OF ELECTROCATALYSTS USING FTACV

This section highlights the use of FTacV in unravelling electrochemical processes, determining the EASD, and quantifying intrinsic properties of catalytic reactions, as well as determining kinetically relevant parameters and processes. This review adds an additional perspective on the use of the FTacV technique for analysis of electrocatalysts. For additional aspects and applications of FTacV, there are several highly recommended review articles available in the literature.^{25,27,54,60,80–82}

3.1. Uncovering Faradaic Processes Not Visible under dc Voltammetry. The ability of FTacV to discriminate between processes with differences in kinetics or linearity of response can be utilized to uncover faradaic processes not visible when using dcV measurements.⁶³ By varying the frequency of the applied sinewave, different processes can be

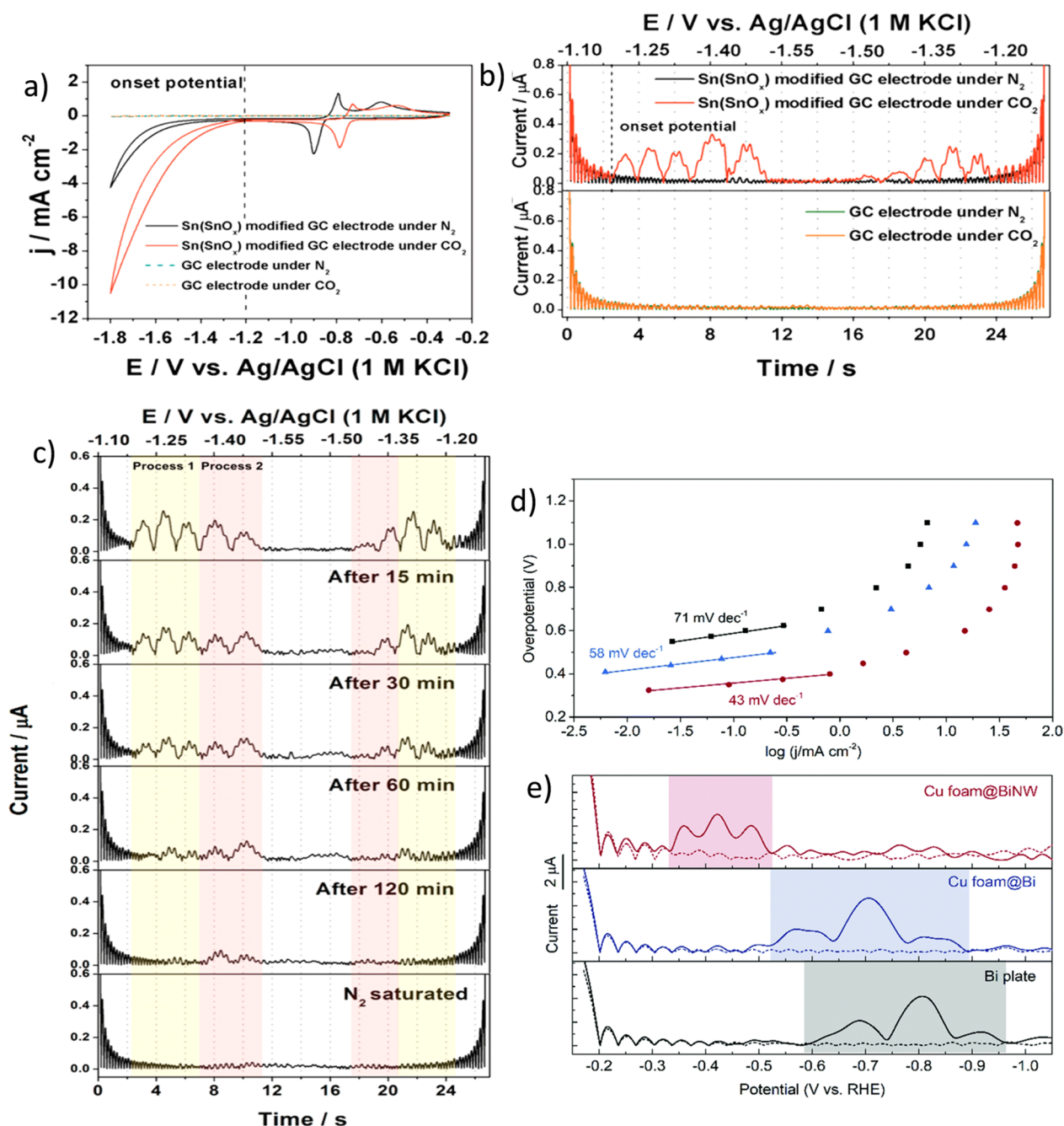


Figure 4. Uncovering faradaic processes not visible by dc voltammetry in CO₂RR catalysts. **a)** dc and **b)** ac voltammograms obtained in 0.5 M NaHCO₃ aqueous electrolyte using a Sn(SnO_x)-modified GC electrode and a bare GC electrode in the presence of CO₂ and N₂. **a)** dc voltammogram showing the onset of the CO₂RR. **b)** Fifth harmonic component extracted from FTacV measurements showing the detection of a faradaic processes under CO₂ turnover conditions. **c)** Fifth harmonic component extracted from FTacV measurements during CO₂RR on a Sn(SnO_x)-modified GC electrode with the concentration of CO₂, decreasing from top (CO₂ saturated solution) to bottom (N₂ saturated solution). Reprinted with permission from ref 32. Copyright American Chemical Society. **d)** Tafel plots and slopes for electrolysis data obtained with Bi plate (black squares) Cu foam@Bi (blue triangles), and Cu foam@BiNW (red dots) electrodes. **e)** Fourth harmonic component extracted from FTacV measurements obtained under CO₂RR turnover conditions from Cu foam@BiNW (top, red), Cu foam@Bi (middle, blue), and Bi (bottom, black) electrodes. Reprinted by permission of the Royal Society of Chemistry from ref 85. Permission conveyed through Copyright Clearance Center, Inc.

separated and quantified.^{69,77,83,84} Adamson et al.²⁸ showed the importance of increasing the frequency in order to discriminate between the faradaic charge-transfer process of surface-confined electrocatalysts and the catalytic current generated in the presence of reactants. They tuned the hydrogen evolution reaction (HER) electrocatalytic activity of NiFe-hydrogenase enzymes by influencing the secondary coordination sphere of the outermost distal [Fe₄S₄]^{2+/+} electron entry/

exit site which transfers electrons between the surface of the protein and the bimetallic NiFe active site. At a sinewave frequency of 9 Hz, the separation between the catalytic and noncatalytic current was not fully clear, and only when increasing the frequency to 144 Hz was a clear noncatalytic harmonic current obtained from the faradaic charge-transfer reaction to the active site. This enabled the authors to extract

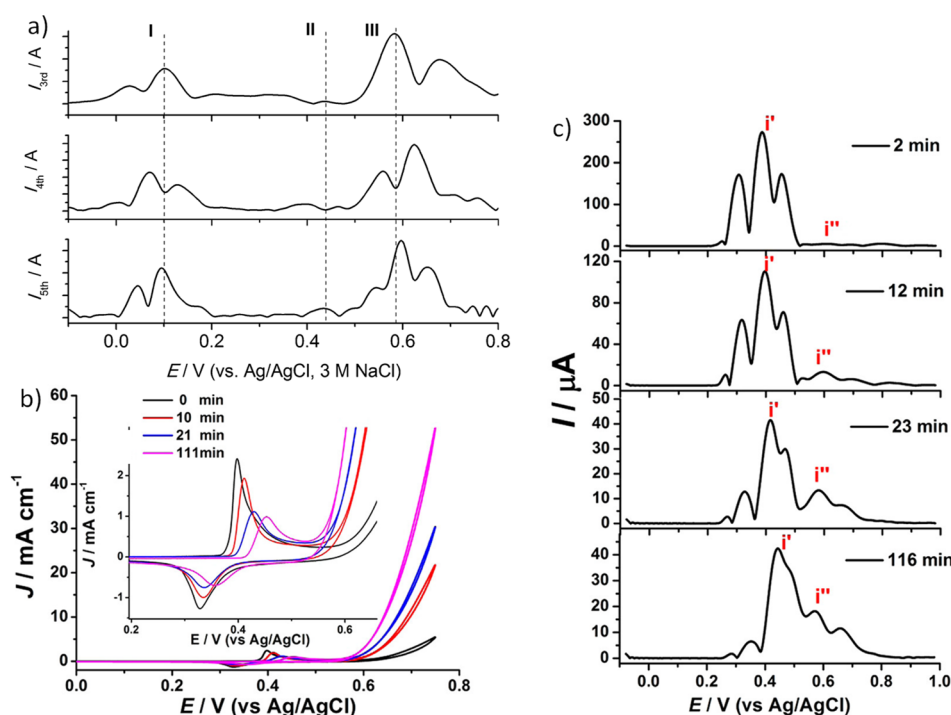


Figure 5. Uncovering faradaic processes not visible under dc voltammetry in OER catalysts. a) Third, fourth, and fifth harmonic components extracted from FTacV measurements obtained with a graphene cobalt nanocomposite modified electrode in aqueous 1 M NaOH electrolyte showing three faradaic processes. Reprinted by permission of the Royal Society of Chemistry from ref 90. Permission conveyed through Copyright Clearance Center, Inc. b) Dc and c) ac voltammograms obtained from a Ni–Nb modified GC electrode showing changes to the activity and redox properties of the catalysts over time with an emergence of a new redox process as the activity increases. Reprinted with permission from ref 91. Copyright American Chemical Society.

the EASD and the TOF, which were later used for activity comparison between different electrocatalysts.

FTacV has been extensively applied to other electrocatalytic systems as well. Zhang et al.³² utilized the high sensitivity of the higher harmonics to probe the mechanism of the CO₂RR on a tin-oxide electrocatalyst. Their results show that under a CO₂ atmosphere two charge-transfer processes emerge in the higher-order harmonic components, that were not observed under an inert atmosphere (N₂) nor under dcV conditions (Figure 4a and b). The relation between the faradaic processes in the harmonics and the presence of CO₂ was further confirmed by CO₂ concentration dependent FTacV measurements, that showed a reduction in the harmonic current as the CO₂ concentration was reduced (Figure 4c). The difference in the rate of change in the harmonic current between the two processes, as the CO₂ concentration changed, led to the conclusion that one process is due to CO₂ and the other to the formation of H₂CO₃ with both being adsorbed on the surface of the electrode. By systematically analyzing the obtained results, they concluded that the faradaic current is due to an inner-sphere electron-transfer step to the adsorbed CO₂, and that the rate determining step is the protonation of the reduced CO₂ radical. A similar rate determining step was found by Zhang et al.,⁵⁰ when analyzing the CO₂RR catalyzed by a bismuth subcarbonate electrode using FTacV. In a follow up work, the same group synthesized lattice-dislocated bismuth nanowires grown on a copper foam as an electrocatalyst for the CO₂RR (Figure 4d and e).⁸⁵ By employing FTacV to analyze and compare the reaction kinetics with different electrocatalysts, it was shown that the rate determining step changes from the protonation of the reduced adsorbed CO₂^{•−} radical, as

is in the case of bismuth metal electrodes, to the reduction of the protonated species when the lattice-dislocated bismuth nanowire is used as a catalyst.

FTacV has been used to experimentally measure and estimate the potentials at which electrochemical transitions occur during catalytic reactions, an important and underutilized ability of such measurements which can be used to compare theoretical calculations of adsorption energies of intermediates with experimentally determined ones.^{10,48,86–89} For example, Guo et al.,⁹⁰ investigated the OER electrocatalytic activity of a graphene-cobalt nanocomposite catalyst electrodeposited on an electrode in alkaline media (pH = 14). By conducting FTacV measurements they were able to distinguish between three faradaic processes at different potentials, one of which has not been detectable under dc conditions in earlier investigations due to the high catalytic current occurring at the relevant potentials (Figure 5a).

FTacV has also been used to follow changes and emergences of new processes occurring over the course of the lifetime of catalysts. Liu et al.,⁹¹ showed an appearance of a faradaic process during the aging of the Ni(OH)₂ catalyst they synthesized for the OER catalysis. They developed a method for the electrodeposition of cobalt and nickel to form nanostructures with the assistance of the Lindqvist ion, [Nb₆O₁₉]^{8−}, and applied the synthesized materials as catalysts for OER electrocatalysis in alkaline media (pH = 14). It was shown that for the Co(OH)₂ catalyst three processes are seen, similar to what has been found in an earlier work by Guo et al.,⁹⁰ while for the Ni(OH)₂ catalyst no processes are seen beyond what is visible from dcV measurements (Figure 5b and c). Interestingly, it was found that an additional oxidation

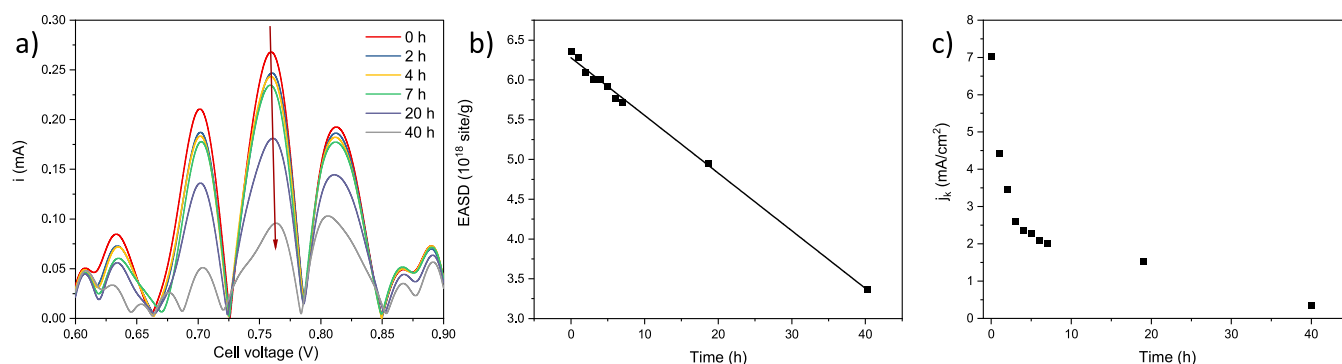


Figure 6. a) *In situ* FTacV measurements conducted during fuel-cell stability tests were used to extract the electrochemical active site density (EASD). b) EASD plotted versus time. c) The current density at 0.8 V extracted from IV measurements and the EASD found from the FTacV can be used to find the average TOF. Reproduced with permission from ref 45.

processes emerges after aging the $\text{Ni}(\text{OH})_2$. This process is not visible in the dcV measurements. The increase in the current of this newly detected process occurs concurrently with a decrease in the harmonic current of the faradaic process seen with the pristine catalyst, and an increase in the catalytic current, which led to the conclusion that the observed redox process is the new formed phase of β -NiOOH, which is more active than the γ -NiOOH phase present in the pristine catalyst. In summary, FTacV can unravel faradaic processes that cannot be detected using traditional dcV measurements.

3.2. Determination of the EASD. As mentioned in the introduction, the intrinsic activity of a catalyst can be assessed by its TOF, which is determined from the kinetic current and EASD. In cases where a redox transition occurs and is directly related to the active sites, e.g., hydrogen underpotential deposition on Pt, the integrated charge under the redox peaks can be used to determine the EASD. However, in many systems, the redox transition peaks may be small or even undetectable in dcV due to high capacitance or a catalytic current that masks the redox transition. To address this challenge, Zhang et al.,⁹² utilized FTacV to extract the number of electroactive sites masked by the catalytic current of the HER. They anchored an oxomolybdate on copper foam, which exhibits HER activity over a large pH range, and used FTacV to probe the redox transition of the $\text{Mo}^{4+/3+}$ and $\text{Mo}^{3+/2+}$ processes. The latter transition is crucial for the HER activity and coincides with the onset of the HER. By comparing their results with simulations, they estimated the surface coverage of active sites and extracted the TOF of the catalytic reaction. Similarly, Snitkoff-Sol et al.,⁴⁵ employed FTacV to discriminate the faradaic current from non-faradaic background currents to measure the EASD of an ORR platinum-group metal-free catalyst *in situ* during fuel-cell testing (Figure 6) by comparing the harmonic components to simulations. They demonstrated that it is possible to determine EASD during stability tests using FTacV and enabled the monitoring of changes in the number of active sites and TOF over time.

3.3. Determination of Reaction Parameters of the Redox Reaction of the Surface Confined Species. The quantification and analysis of the kinetic and thermodynamic parameters of active-sites in surface-confined catalysts is crucial for understating catalytic activity.⁹³ Zouraris et al.⁹⁴ developed a methodology that employs theoretical calculations to provide an initial estimate of the rate constant for an electron-transfer reaction to surface-confined species. By conducting multiple FTacV measurements at different frequencies and identifying

the range where the reaction exhibits quasi-reversibility, one can extract an estimate of the rate constant from a simulated plot of peak current vs the normalized rate constant (Figure 7a). Zouraris et al.⁹⁵ used this methodology to estimate the rate constant of a redox enzyme, lytic polysaccharide monooxygenase, that was immobilized on an electrode. This study demonstrated that this methodology is applicable for the initial estimation of the kinetic parameters of redox reactions.

3.4. Determination of Kinetic and Thermodynamic Parameters of the Catalytic Reaction. Understanding the reaction mechanism of catalytic reactions is crucial to the development of better catalysts. Voltammetry-based methods have a strong record of successes in revealing catalytic mechanisms.^{88,96–101} The use of the higher-order harmonic components extracted from FTacV measurements for the analysis of catalytic reactions has many advantages, such as the high discrimination between linear and nonlinear processes, and the tunability of the probing time scale. The high sensitivity of the harmonics to changes in the kinetics increases the identifiability of parameters and facilitates data analysis,⁷⁰ making the FTacV technique especially suitable for integrating microkinetic models and comparing the experimental harmonic components to simulated ones. For example, Bonke et al.,⁴⁸ employed FTacV with a simplified microkinetic model for the OER to quantitatively analyze the catalytic activity of CoO_x , MnO_x , and NiO_x electrocatalysts in 0.1 M borate buffer (pH = 9.2). They systematically varied the surface coverage of the three catalysts, and by extensively analyzing the higher harmonics extracted from FTacV measurements, they determined the underlying faradaic charge-transfer processes that control the rate of the OER with these catalysts for the first time (Figure 7b). Their methodology, i.e., using a microkinetic model and comparing the simulated harmonics to experimental ones to extract kinetic parameters, can be used to compare catalysts and to understand the nature of possible differences in activity that may be too subtle to be discerned from dcV measurements. The sensitivity of the higher harmonics of the FTacV measurements can be utilized and compared with detailed microkinetic models and may enable the quantification of adsorption energies which are currently mostly available through quantum mechanical calculations. It is noteworthy that in a later work, King et al.,¹⁰² used the redox potentials found for the different faradaic processes in the FTacV measurements to guide *in situ* X-ray absorption measurements of the OER on CoO_x catalysts. Their results confirm the estimated magnitudes of the rate constants found

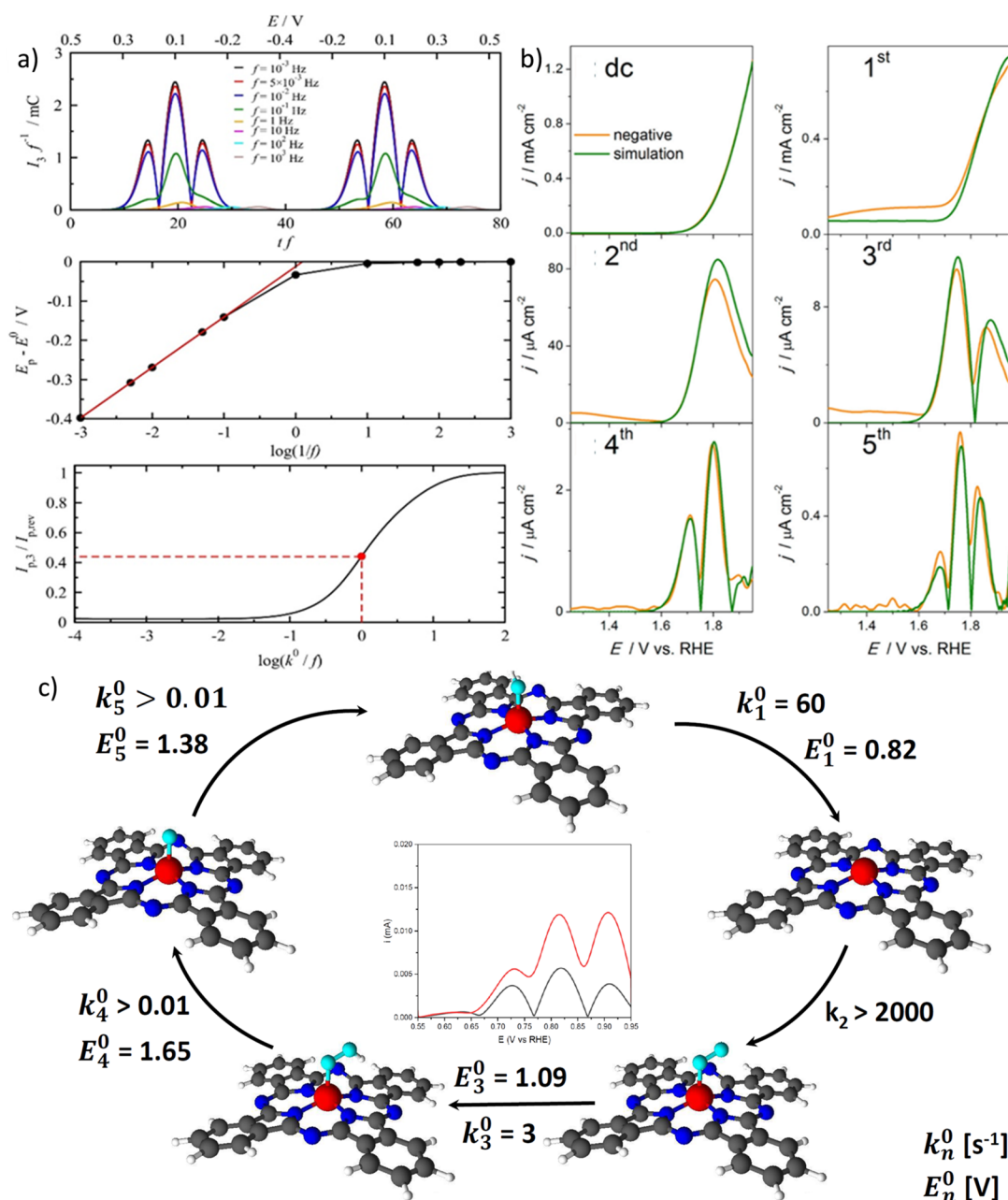


Figure 7. Determination of kinetic and thermodynamic parameters. **a)** Methodology for determining thermodynamic and kinetic parameters of a surface-confined redox species: **Top**, third harmonic components extracted from FTacV simulations for different frequencies (f) to determine the reversible potential (E^0) and principal peak current (I_p). The y-axis is the current divided by frequency and the x-axis is given by time multiplied by the frequency. **Middle**, shift of the potential of the principal peak for the determination of the transfer coefficient. The y-axis is the peak potential of the principal peaks versus the reversible potential and the x-axis is minus the logarithm of the frequency. **Bottom**, dependence of the normalized principal peak height on the ratio of the heterogeneous rate constant (k^0) to the frequency to estimate k^0 . The y-axis is the peak current of the third harmonic simulated with a specific heterogeneous rate constant normalized to the peak current of the reversible case and the x-axis is the logarithm of the ratio of the heterogeneous rate constant and applied frequency. Reprinted from ref 94 with permission from Elsevier. **b)** Comparison of experimental (orange) and simulated FTacV data for OER catalyzed by CoO_x catalysts. Reprinted with permission from ref 48. Copyright American Chemical Society. **c)** Scheme of the reaction parameters found for the proposed reaction mechanism of the ORR on an iron-phthalocyanine PGM-free catalysts. The harmonic currents depicted in the middle of the scheme are the fifth harmonic components measured at a frequency of 0.98 Hz in the presence (red) and absence (black) of O_2 . Reproduced with permission from ref 104.

in the work of Bonke et al.⁴⁸ highlighting the importance of such endeavors. Vodeb et al. followed a similar methodology and gained valuable insights on the catalysis of OER in acidic media with precious metal catalysts.¹⁰³ They compared between different Ir-based catalysts, probing the kinetic and thermodynamic reaction parameters by comparing the higher harmonic components to a detailed microkinetic model

enabling them to draw mechanistic conclusions on the differences in activity between the catalysts. Recently, Snitk-off-Sol et al. investigated the ORR with a PGM-free catalyst.¹⁰⁴ They extracted relevant reaction parameters by taking advantage of the high kinetic sensitivity of the harmonic components generated from FTacV measurements conducted over a range of frequencies (Figure 7c). The reaction

parameters were found by comparing the harmonics to a detailed microkinetic model and then were used to simulate steady-state experiments which are much less sensitive to the reaction parameters in the model compared to FTacV measurements, strengthening the validity of the drawn mechanistic conclusions.

4. CONCLUSIONS AND OUTLOOK

As the applications of electrocatalysis broaden toward new\old domains such as electrification of the chemical industry, the need for accurate, quantitative, and sensitive measures of the underlying mechanisms and roots of the catalytic activity becomes acute. Although FTacV is well-established as a highly sensitive electroanalytical technique, it is not yet widespread in the electrocatalysis community. In this review we have highlighted the exciting and unparalleled insights available from the use of FTacV in the analysis of electrocatalytic reactions. While more traditional techniques for analysis of electrocatalysis, such as dcV, electrochemical impedance spectroscopy, and steady-state rotating-disc (ring)-electrodes are indispensable for catalytic activity analyses, the high kinetic sensitivity of the harmonic components makes FTacV an additional, highly suitable technique for fundamental mechanistic investigations. Going forward, statistical analysis of the reaction parameters extracted via model-experiment comparison of FTacV measurements will enable estimating inherent errors in the models, providing insights into the extracted parameters. This may eventually lead to the development and application of hypothesis testing methods in the field of electrocatalysis, where competing models are compared using the tools of Bayesian inference, as well as the use of optimal experimental designs to increase the validity of mechanistic insights.

AUTHOR INFORMATION

Corresponding Author

Lior Elbaz – Department of Chemistry, Bar-Ilan Center for Nanotechnology and Advanced Materials, Bar-Ilan University, Ramat-Gan 5290002, Israel; orcid.org/0000-0003-4989-5135; Email: lior.elbaz@biu.ac.il

Authors

Rafael Z. Snitkoff-Sol – Department of Chemistry, Bar-Ilan Center for Nanotechnology and Advanced Materials, Bar-Ilan University, Ramat-Gan 5290002, Israel; orcid.org/0000-0001-6550-2878

Alan M. Bond – School of Chemistry, Monash University, Clayton, Victoria 3800, Australia; orcid.org/0000-0002-1113-5205

Complete contact information is available at:
<https://pubs.acs.org/10.1021/acscatal.4c01526>

Notes

The authors declare no competing financial interest.

REFERENCES

- (1) Seh, Z. W.; Kibsgaard, J.; Dickens, C. F.; Chorkendorff, I.; Nørskov, J. K.; Jaramillo, T. F. Combining theory and experiment in electrocatalysis: Insights into materials design. *Science* **2017**, 355 (6321), No. eaad4998.
- (2) Eikerling, M.; Kulikovskiy, A. *Polymer Electrolyte Fuel Cells*; CRC Press: Boca Raton, 2015.
- (3) Chatenet, M.; Pollet, B. G.; Dekel, D. R.; Dionigi, F.; Deseure, J.; Millet, P.; Braatz, R. D.; Bazant, M. Z.; Eikerling, M.; Staffell, I.; Balcombe, P.; Shao-Horn, Y.; Schäfer, H. Water electrolysis: from textbook knowledge to the latest scientific strategies and industrial developments. *Chem. Soc. Rev.* **2022**, 51 (11), 4583–4762.
- (4) Singh, N.; Goldsmith, B. R. Role of Electrocatalysis in the Remediation of Water Pollutants. *ACS Catal.* **2020**, 10 (5), 3365–3371.
- (5) Novaes, L. F.; Liu, J.; Shen, Y.; Lu, L.; Meinhardt, J. M.; Lin, S. Electrocatalysis as an enabling technology for organic synthesis. *Chem. Soc. Rev.* **2021**, 50 (14), 7941–8002.
- (6) Barton, J. L. Electrification of the chemical industry. *Science* **2020**, 368 (6496), 1181–1182.
- (7) Papanikolaou, G.; Centi, G.; Perathoner, S.; Lanzafame, P. Catalysis for e-Chemistry: Need and Gaps for a Future De-Fossilized Chemical Production, with Focus on the Role of Complex (Direct) Syntheses by Electrocatalysis. *ACS Catal.* **2022**, 12 (5), 2861–2876.
- (8) Oldham, K.; Myland, J.; Bond, A. *Electrochemical Science and Technology: Fundamentals and Applications*; John Wiley & Sons, 2011.
- (9) Nørskov, J. K.; Studt, F.; Abild-Pedersen, F.; Bligaard, T. *Fundamental Concepts in Heterogeneous Catalysis*; John Wiley & Sons, 2014.
- (10) Koper, M. T. Thermodynamic theory of multi-electron transfer reactions: Implications for electrocatalysis. *J. Electroanal. Chem.* **2011**, 660 (2), 254–260.
- (11) Kulkarni, A.; Siahrostami, S.; Patel, A.; Nørskov, J. K. Understanding Catalytic Activity Trends in the Oxygen Reduction Reaction. *Chem. Rev.* **2018**, 118 (5), 2302–2312.
- (12) Hansen, H. A.; Viswanathan, V.; Nørskov, J. K. Unifying kinetic and thermodynamic analysis of 2 e- and 4 e-reduction of oxygen on metal surfaces. *J. Phys. Chem. C* **2014**, 118 (13), 6706–6718.
- (13) Nørskov, J. K.; Rossmeisl, J.; Logadottir, A.; Lindqvist, L.; Kitchin, J. R.; Bligaard, T.; Jónsson, H. Origin of the Overpotential for Oxygen Reduction at a Fuel-Cell Cathode. *J. Phys. Chem. B* **2004**, 108 (46), 17886–17892.
- (14) Dickens, C. F.; Kirk, C.; Nørskov, J. K. Insights into the Electrochemical Oxygen Evolution Reaction with ab Initio Calculations and Microkinetic Modeling: Beyond the Limiting Potential Volcano. *J. Phys. Chem. C* **2019**, 123 (31), 18960–18977.
- (15) Kelly, S. R.; Kirk, C.; Chan, K.; Nørskov, J. K. Electric Field Effects in Oxygen Reduction Kinetics: Rationalizing pH Dependence at the Pt(111), Au(111), and Au(100) Electrodes. *J. Phys. Chem. C* **2020**, 124 (27), 14581–14591.
- (16) Exner, K. S. Why the microkinetic modeling of experimental tafel plots requires knowledge of the reaction intermediate's binding energy. *Electrochem. Sci. Adv.* **2022**, 2, No. e2100037.
- (17) Exner, K. S. Why approximating electrocatalytic activity by a single free-energy change is insufficient. *Electrochim. Acta* **2021**, 375, 137975.
- (18) Exner, K. S.; Sohrabnejad-Eskan, I.; Over, H. A universal approach to determine the free energy diagram of an electrocatalytic reaction. *ACS Catal.* **2018**, 8 (3), 1864–1879.
- (19) Exner, K. S.; Over, H. Kinetics of electrocatalytic reactions from first-principles: a critical comparison with the ab initio thermodynamics approach. *Accounts of chemical research* **2017**, 50 (5), 1240–1247.
- (20) Exner, K. S. Is Thermodynamics a Good Descriptor for the Activity? Re-Investigation of Sabatier's Principle by the Free Energy Diagram in Electrocatalysis. *ACS Catal.* **2019**, 9 (6), 5320–5329.
- (21) Exner, K. S.; Over, H. Beyond the Rate-Determining Step in the Oxygen Evolution Reaction over a Single-Crystalline IrO₂(110) Model Electrode: Kinetic Scaling Relations. *ACS Catal.* **2019**, 9 (8), 6755–6765.
- (22) Huang, J.; Zhu, X.; Eikerling, M. The rate-determining term of electrocatalytic reactions with first-order kinetics. *Electrochim. Acta* **2021**, 393, 139019.
- (23) Zhang, Y.; Huang, J.; Eikerling, M. Criterion for finding the optimal electrocatalyst at any overpotential. *Electrochim. Acta* **2021**, 400, 139413.

- (24) Govindarajan, N.; Kastlunger, G.; Heenen, H. H.; Chan, K. Improving the intrinsic activity of electrocatalysts for sustainable energy conversion: where are we and where can we go? *Chemical Science* **2021**, *13* (1), 14–26.
- (25) Changing the Look of Voltammetry. *Anal. Chem.* **2005**, *77* (9), 186–195.
- (26) Gavaghan, D. J.; Bond, A. M. A complete numerical simulation of the techniques of alternating current linear sweep and cyclic voltammetry: analysis of a reversible process by conventional and fast Fourier transform methods. *J. Electroanal. Chem.* **2000**, *480* (1), 133–149.
- (27) Adamson, H.; Bond, A. M.; Parkin, A. Probing biological redox chemistry with large amplitude Fourier transformed ac voltammetry. *Chem. Commun.* **2017**, *53* (69), 9519–9533.
- (28) Adamson, H.; Robinson, M.; Wright, J. J.; Flanagan, L. A.; Walton, J.; Elton, D.; Gavaghan, D. J.; Bond, A. M.; Roessler, M. M.; Parkin, A. Retuning the Catalytic Bias and Overpotential of a [NiFe]-Hydrogenase via a Single Amino Acid Exchange at the Electron Entry/Exit Site. *J. Am. Chem. Soc.* **2017**, *139* (31), 10677–10686.
- (29) Adamson, H.; Robinson, M.; Bond, P. S.; Soboh, B.; Gillow, K.; Simonov, A. N.; Elton, D. M.; Bond, A. M.; Sawers, R. G.; Gavaghan, D. J.; Parkin, A. Analysis of HypD Disulfide Redox Chemistry via Optimization of Fourier Transformed ac Voltammetric Data. *Anal. Chem.* **2017**, *89* (3), 1565–1573.
- (30) Zouraris, D. *Electrochemical study of redox enzymes and their utilization on modified electrodes*. PhD Thesis, National Technical University of Athens, 2021.
- (31) Hodgetts, R. Y.; Du, H.-L.; Nguyen, T. D.; MacFarlane, D.; Simonov, A. N. Electrocatalytic Oxidation of Hydrogen as an Anode Reaction for the Li-Mediated N₂ Reduction to Ammonia. *ACS Catal.* **2022**, *12* (9), 5231–5246.
- (32) Zhang, Y.; Chen, L.; Li, F.; Easton, C. D.; Li, J.; Bond, A. M.; Zhang, J. Direct Detection of Electron Transfer Reactions Underpinning the Tin-Catalyzed Electrochemical Reduction of CO₂ using Fourier-Transformed ac Voltammetry. *ACS Catal.* **2017**, *7* (7), 4846–4853.
- (33) Abdul-Rahim, O.; Simonov, A. N.; Boas, J. F.; R  ther, T.; Collins, D. J.; Perlmutter, P.; Bond, A. M. Studies on the nuances of the electrochemically induced room temperature isomerization of cis-stilbene in acetonitrile and ionic liquids. *J. Phys. Chem. B* **2014**, *118* (11), 3183–3191.
- (34) Rahman, M. A.; Guo, S.-X.; Laurans, M.; Izzet, G.; Proust, A.; Bond, A. M.; Zhang, J. Thermodynamics, electrode kinetics, and mechanistic nuances associated with the voltammetric reduction of dissolved [n-Bu₄N]⁺ 4 [PW₁₁O₃₉ {Sn (C₆H₄) C≡C (C₆H₄)-(N₃C₄H₁₀)}] and a surface-confined diazonium derivative. *ACS Applied Energy Materials* **2020**, *3* (4), 3991–4006.
- (35) Usov, P. M.; Simonov, A. N.; Bond, A. M.; Murphy, M. J.; D'Alessandro, D. M. Untangling complex redox chemistry in zeolitic imidazolate frameworks using Fourier transformed alternating current voltammetry. *Analytical chemistry* **2017**, *89* (19), 10181–10187.
- (36) Li, J.; Kennedy, G. F.; Bond, A. M.; Zhang, J. Demonstration of Superiority of the Marcus-Hush Electrode Kinetic Model in the Electrochemistry of Dissolved Decamethylferrocene at a Gold-Modified Electrode by Fourier-Transformed Alternating Current Voltammetry. *J. Phys. Chem. C* **2018**, *122* (16), 9009–9014.
- (37) Bullock, J. P.; Mashkina, E.; Bond, A. M. Activation parameters derived from a temperature dependent large amplitude ac voltammetric study of the electrode kinetics of the Cp₂M^{0/+} redox couples (M = Fe, Co) at a glassy carbon electrode. *J. Phys. Chem. A* **2011**, *115* (24), 6493–6502.
- (38) Nakanishi, B. R.; Allanore, A. Electrochemical study of a pendant molten alumina droplet and its application for thermodynamic property measurements of Al-Ir. *J. Electrochem. Soc.* **2017**, *164* (13), No. E460.
- (39) Caldwell, A. H.; Allanore, A. Alternating current voltammetry of electrode reactions with constant surface activity: Application to electrolysis of molten electrolytes. *J. Electroanal. Chem.* **2020**, *861*, 113709.
- (40) Sokhanvaran, S.; Lee, S.-K.; Lambotte, G.; Allanore, A. Electrochemistry of molten sulfides: copper extraction from BaS-Cu₂S. *J. Electrochem. Soc.* **2016**, *163* (3), D115.
- (41) Fabian, C. P.; Le, T. H.; Bond, A. M. Cyclic Voltammetric Experiment-Simulation Comparisons of the Complex Zr⁴⁺ to ZrO Reduction Mechanism at a Molybdenum Electrode in LiF-CaF₂ Eutectic Molten Salt. *J. Electrochem. Soc.* **2022**, *169* (3), 036506.
- (42) Lucio, A. J.; Shaw, S. K.; Zhang, J.; Bond, A. M. Large-Amplitude Fourier-Transformed AC Voltammetric Study of the Capacitive Electrochemical Behavior of the 1-Butyl-3-methylimidazolium Tetrafluoroborate-Polycrystalline Gold Electrode Interface. *J. Phys. Chem. C* **2017**, *121* (22), 12136–12147.
- (43) Bentley, C. L.; Li, J.; Bond, A. M.; Zhang, J. Mass-transport and heterogeneous electron-transfer kinetics associated with the ferrocene/ferrocenium process in ionic liquids. *J. Phys. Chem. C* **2016**, *120* (30), 16516–16525.
- (44) Shiddiky, M. J.; Torriero, A. A.; Zhao, C.; Burgar, I.; Kennedy, G.; Bond, A. M. Nonadditivity of faradaic currents and modification of capacitance currents in the voltammetry of mixtures of ferrocene and the cobaltocenium cation in protic and aprotic ionic liquids. *J. Am. Chem. Soc.* **2009**, *131* (23), 7976–7989.
- (45) Snitkoff-Sol, R. Z.; Friedman, A.; Honig, H. C.; Yurko, Y.; Kozhushner, A.; Zachman, M. J.; Zelenay, P.; Bond, A. M.; Elbaz, L. Quantifying the electrochemical active site density of precious metal-free catalysts in situ in fuel cells. *Nature Catalysis* **2022**, *5* (2), 163–170.
- (46) Snitkoff-Sol, R. Z.; Elbaz, L. Assessing and measuring the active site density of PGM-free ORR catalysts. *J. Solid State Electrochem.* **2022**, *26*, 1839.
- (47) Lee, C.-Y.; Guo, S.-X.; Murphy, A. F.; McCormac, T.; Zhang, J.; Bond, A. M.; Zhu, G.; Hill, C. L.; Geletii, Y. V. Detailed electrochemical studies of the tetraruthenium polyoxometalate water oxidation catalyst in acidic media: identification of an extended oxidation series using fourier transformed alternating current voltammetry. *Inorg. Chem.* **2012**, *51* (21), 11521–11532.
- (48) Bonke, S. A.; Bond, A. M.; Spiccia, L.; Simonov, A. N. Parameterization of Water Electrooxidation Catalyzed by Metal Oxides Using Fourier Transformed Alternating Current Voltammetry. *J. Am. Chem. Soc.* **2016**, *138* (49), 16095–16104.
- (49) Sun, C.; Li, F.; An, H.; Li, Z.; Bond, A. M.; Zhang, J. Facile electrochemical co-deposition of metal (Cu, Pd, Pt, Rh) nanoparticles on reduced graphene oxide for electrocatalytic reduction of nitrate/nitrite. *Electrochim. Acta* **2018**, *269*, 733–741.
- (50) Zhang, Y.; Zhang, X.; Ling, Y.; Li, F.; Bond, A. M.; Zhang, J. Controllable synthesis of few-layer bismuth subcarbonate by electrochemical exfoliation for enhanced CO₂ reduction performance. *Angew. Chem.* **2018**, *130* (40), 13467–13471.
- (51) Chen, L.; Li, F.; Bentley, C. L.; Horne, M.; Bond, A. M.; Zhang, J. Electrochemical reduction of CO₂ with an oxide-derived lead nanocorralline electrode in dimcarb. *ChemElectroChem.* **2017**, *4* (6), 1402–1410.
- (52) Zheng, F. *Advanced Electrochemical Analysis for Complex Electrode Applications*. PhD Thesis, University of Cambridge, 2019.
- (53) Lertanantawong, B.; O'Mullane, A. P.; Surareungchai, W.; Somasundrum, M.; Burke, L. D.; Bond, A. M. Study of the underlying electrochemistry of polycrystalline gold electrodes in aqueous solution and electrocatalysis by large amplitude Fourier transformed alternating current voltammetry. *Langmuir* **2008**, *24* (6), 2856–2868.
- (54) Kennedy, G. F.; Bond, A. M.; Simonov, A. N. Modelling ac voltammetry with MECSim: facilitating simulation-experiment comparisons. *Current Opinion in Electrochemistry* **2017**, *1* (1), 140–147.
- (55) <http://www.garethkennedy.net/MECSim.html> (accessed on April 8, 2024).
- (56) Gundry, L.; Guo, S.-X.; Kennedy, G.; Keith, J.; Robinson, M.; Gavaghan, D.; Bond, A. M.; Zhang, J. Recent advances and future perspectives for automated parameterisation, Bayesian inference and machine learning in voltammetry. *Chem. Commun.* **2021**, *57* (15), 1855–1870.

- (57) Gundry, L.; Kennedy, G.; Keith, J.; Robinson, M.; Gavaghan, D.; Bond, A. M.; Zhang, J. A Comparison of Bayesian Inference Strategies for Parameterisation of Large Amplitude AC Voltammetry Derived from Total Current and Fourier Transformed Versions. *ChemElectroChem* **2021**, *8* (12), 2238–2258.
- (58) Li, J.; Kennedy, G. F.; Gundry, L.; Bond, A. M.; Zhang, J. Application of Bayesian Inference in Fourier-Transformed Alternating Current Voltammetry for Electrode Kinetic Mechanism Distinction. *Analytical chemistry* **2019**, *91* (8), 5303–5309.
- (59) Alévêque, O.; Levillain, E.; Morille, Y. Alternative voltammetry on self-assembled monolayers: An original approach to estimate the electrochemical electron-transfer rate constants when electroactive adsorbed species interact. *J. Electroanal. Chem.* **2020**, *873*, 114414.
- (60) Guo, S.-X.; Bentley, C. L.; Kang, M.; Bond, A. M.; Unwin, P. R.; Zhang, J. Advanced Spatiotemporal Voltammetric Techniques for Kinetic Analysis and Active Site Determination in the Electrochemical Reduction of CO₂. *Acc. Chem. Res.* **2022**, *55* (3), 241–251.
- (61) Honeychurch, M. J.; Rechnitz, G. A. About the Formulation of Charge Transfer Processes Occurring with Adsorbed Species. *Electroanalysis* **1999**, *11* (12), 907–908.
- (62) Honeychurch, M. J.; Rechnitz, G. A. Voltammetry of Adsorbed Molecules. Part 1: Reversible Redox Systems. *Electroanalysis* **1998**, *10* (5), 285–293.
- (63) Zhang, J.; Bond, A. M. Theoretical studies of large amplitude alternating current voltammetry for a reversible surface-confined electron transfer process coupled to a pseudo first-order electrocatalytic process. *J. Electroanal. Chem.* **2007**, *600* (1), 23–34.
- (64) FTacV Surface Confined Educational Simulation. https://github.com/Smittkoff-Sol/FTacV_SC_Simulation.
- (65) Friedman, A.; Smittkoff-Sol, R. Z.; Honig, H. C.; Elbaz, L. Simplified FTacV model to quantify the electrochemically active site density in PGM-free ORR catalysts. *Electrochim. Acta* **2023**, *463*, 142865.
- (66) HRview. <https://github.com/friedmanariel/HRview> (accessed on April 8, 2024).
- (67) Sher, A. A.; Bond, A. M.; Gavaghan, D. J.; Harriman, K.; Feldberg, S. W.; Duffy, N. W.; Guo, S.-X.; Zhang, J. Resistance, capacitance, and electrode kinetic effects in fourier-transformed large-amplitude sinusoidal voltammetry: Emergence of powerful and intuitively obvious tools for recognition of patterns of behavior. *Analytical chemistry* **2004**, *76* (21), 6214–6228.
- (68) Mashkina, E.; Bond, A. M. Implementation of a statistically supported heuristic approach to alternating current voltammetric harmonic component analysis: Re-evaluation of the macrodisk glassy carbon electrode kinetics for oxidation of ferrocene in acetonitrile. *Analytical chemistry* **2011**, *83* (5), 1791–1799.
- (69) Bano, K.; Zhang, J.; Bond, A. M. Investigations of Fast Electrode Kinetics for Reduction of 2,3,5,6-Tetrafluoro-7,7,8,8-tetracyanoquinodimethane in Conventional Solvents and Ionic Liquids Using Fourier Transformed Large Amplitude Alternating Current Voltammetry. *J. Phys. Chem. C* **2014**, *118* (18), 9560–9569.
- (70) Gavaghan, D. J.; Cooper, J.; Daly, A. C.; Gill, C.; Gillow, K.; Robinson, M.; Simonov, A. N.; Zhang, J.; Bond, A. M. Use of Bayesian Inference for Parameter Recovery in DC and AC Voltammetry. *ChemElectroChem* **2018**, *5* (6), 917–935.
- (71) Bond, A. M.; Duffy, N. W.; Elton, D. M.; Fleming, B. D. Characterization of nonlinear background components in voltammetry by use of large amplitude periodic perturbations and Fourier transform analysis. *Analytical chemistry* **2009**, *81* (21), 8801–8808.
- (72) Stevenson, G. P.; Lee, C.-Y.; Kennedy, G. F.; Parkin, A.; Baker, R. E.; Gillow, K.; Armstrong, F. A.; Gavaghan, D. J.; Bond, A. M. Theoretical analysis of the two-electron transfer reaction and experimental studies with surface-confined cytochrome c peroxidase using large-amplitude Fourier transformed AC voltammetry. *Langmuir* **2012**, *28* (25), 9864–9877.
- (73) Lee, C.-Y.; Stevenson, G. P.; Parkin, A.; Roessler, M. M.; Baker, R. E.; Gillow, K.; Gavaghan, D. J.; Armstrong, F. A.; Bond, A. M. Theoretical and experimental investigation of surface-confined two-center metalloproteins by large-amplitude Fourier transformed ac voltammetry. *Journal of electroanalytical chemistry* **2011**, *656* (1–2), 293–303.
- (74) Simonov, A. N.; Morris, G. P.; Mashkina, E. A.; Bethwaite, B.; Gillow, K.; Baker, R. E.; Gavaghan, D. J.; Bond, A. M. Inappropriate use of the quasi-reversible electrode kinetic model in simulation-experiment comparisons of voltammetric processes that approach the reversible limit. *Analytical chemistry* **2014**, *86* (16), 8408–8417.
- (75) Lloyd-Laney, H. O.; Robinson, M. J.; Bond, A. M.; Parkin, A.; Gavaghan, D. J. A Spotter's Guide to Dispersion in Non-Catalytic Surface-Confined Voltammetry Experiments. *J. Electroanal. Chem.* **2021**, *894*, 115204.
- (76) Tan, S.-y.; Unwin, P. R.; Macpherson, J. V.; Zhang, J.; Bond, A. M. Probing Electrode Heterogeneity Using Fourier-Transformed Alternating Current Voltammetry: Application to a Dual-Electrode Configuration. *Anal. Chem.* **2017**, *89* (5), 2830–2837.
- (77) Li, J.; Bentley, C. L.; Bond, A. M.; Zhang, J. Dual-Frequency Alternating Current Designer Waveform for Reliable Voltammetric Determination of Electrode Kinetics Approaching the Reversible Limit. *Anal. Chem.* **2016**, *88* (4), 2367–2374.
- (78) Morris, G. P.; Baker, R. E.; Gillow, K.; Davis, J. J.; Gavaghan, D. J.; Bond, A. M. Theoretical Analysis of the Relative Significance of Thermodynamic and Kinetic Dispersion in the dc and ac Voltammetry of Surface-Confined Molecules. *Langmuir* **2015**, *31* (17), 4996–5004.
- (79) Lloyd-Laney, H. O.; Yates, N. D. J.; Robinson, M. J.; Hewson, A. R.; Branch, J.; Hemsworth, G. R.; Bond, A. M.; Parkin, A.; Gavaghan, D. J. Recovering biological electron transfer reaction parameters from multiple protein film voltammetric techniques informed by Bayesian inference. *J. Electroanal. Chem.* **2023**, *935*, 117264.
- (80) Zhang, Y.; Simonov, A. N.; Zhang, J.; Bond, A. M. Fourier transformed alternating current voltammetry in electromaterials research: Direct visualisation of important underlying electron transfer processes. *Current Opinion in Electrochemistry* **2018**, *10*, 72–81.
- (81) Bond, A. M.; Elton, D.; Guo, S.-X.; Kennedy, G. F.; Mashkina, E.; Simonov, A. N.; Zhang, J. An integrated instrumental and theoretical approach to quantitative electrode kinetic studies based on large amplitude Fourier transformed a.c. voltammetry: A mini review. *Electrochem. Commun.* **2015**, *57*, 78–83.
- (82) Guo, S.-X.; Bond, A. M.; Zhang, J. Fourier transformed large amplitude alternating current voltammetry: principles and applications. *Review of Polarography* **2015**, *61* (1), 21–32.
- (83) Simonov, A. N.; Grosse, W.; Mashkina, E. A.; Bethwaite, B.; Tan, J.; Abramson, D.; Wallace, G. G.; Moulton, S. E.; Bond, A. M. New insights into the analysis of the electrode kinetics of flavin adenine dinucleotide redox center of glucose oxidase immobilized on carbon electrodes. *Langmuir* **2014**, *30* (11), 3264–3273.
- (84) Tan, S.-y.; Unwin, P. R.; Macpherson, J. V.; Zhang, J.; Bond, A. M. Probing Electrode Heterogeneity using Fourier-Transformed Alternating Current Voltammetry: Protocol Development. *Electrochim. Acta* **2017**, *240*, 514–521.
- (85) Zhang, X.; Sun, X.; Guo, S.-X.; Bond, A. M.; Zhang, J. Formation of lattice-dislocated bismuth nanowires on copper foam for enhanced electrocatalytic CO₂ reduction at low overpotential. *Energy Environ. Sci.* **2019**, *12* (4), 1334–1340.
- (86) Koper, M. T. Theory of multiple proton-electron transfer reactions and its implications for electrocatalysis. *Chemical science* **2013**, *4* (7), 2710–2723.
- (87) Zhou, D.; Wei, J.; He, Z.-D.; Xu, M.-L.; Chen, Y.-X.; Huang, J. Combining single crystal experiments and microkinetic modeling in disentangling thermodynamic, kinetic, and double-layer factors influencing oxygen reduction. *J. Phys. Chem. C* **2020**, *124* (25), 13672–13678.
- (88) Geppert, J.; Röse, P.; Czióska, S.; Escalera-López, D.; Boubnov, A.; Saraçi, E.; Cherevko, S.; Grunwaldt, J.-D.; Krewer, U. Microkinetic Analysis of the Oxygen Evolution Performance at Different Stages of Iridium Oxide Degradation. *J. Am. Chem. Soc.* **2022**, *144* (29), 13205–13217.

- (89) Geppert, J.; Röse, P.; Pauer, S.; Krewer, U. Microkinetic Barriers of the Oxygen Evolution on the Oxides of Iridium, Ruthenium and their Binary Mixtures. *ChemElectroChem* **2022**, *9* (20), No. e202200481.
- (90) Guo, S.-X.; Liu, Y.; Bond, A. M.; Zhang, J.; Karthik, P. E.; Maheshwaran, I.; Kumar, S. S.; Phani, K. L. N. Facile electrochemical co-deposition of a graphene-cobalt nanocomposite for highly efficient water oxidation in alkaline media: direct detection of underlying electron transfer reactions under catalytic turnover conditions. *Phys. Chem. Chem. Phys.* **2014**, *16* (35), 19035–19045.
- (91) Liu, Y.; Guo, S.-X.; Ding, L.; Ohlin, C. A.; Bond, A. M.; Zhang, J. Lindqvist polyoxoniobate ion-assisted electrodeposition of cobalt and nickel water oxidation catalysts. *ACS Appl. Mater. Interfaces* **2015**, *7* (30), 16632–16644.
- (92) Zhang, X.; Zhang, Y.; Li, F.; Easton, C. D.; Bond, A. M.; Zhang, J. Oxomolybdate anchored on copper for electrocatalytic hydrogen production over the entire pH range. *Applied Catalysis B: Environmental* **2019**, *249*, 227–234.
- (93) Zagal, J. H.; Koper, M. T. Reactivity descriptors for the activity of molecular MN4 catalysts for the oxygen reduction reaction. *Angew. Chem., Int. Ed.* **2016**, *55* (47), 14510–14521.
- (94) Zouraris, D.; Karantonis, A. Determination of kinetic and thermodynamic parameters from large amplitude Fourier transform ac voltammetry of immobilized electroactive species. *J. Electroanal. Chem.* **2020**, *876*, 114729.
- (95) Zouraris, D.; Karnaouri, A.; Xydou, R.; Topakas, E.; Karantonis, A. Exploitation of Enzymes for the Production of Biofuels: Electrochemical Determination of Kinetic Parameters of LPMOs. *Applied Sciences* **2021**, *11* (11), 4715.
- (96) Haisch, T.; Kubannek, F.; Nikitina, L.; Nikitin, I.; Pott, S.; Clees, T.; Krewer, U. The origin of the hysteresis in cyclic voltammetric response of alkaline methanol electrooxidation. *Phys. Chem. Chem. Phys.* **2020**, *22* (29), 16648–16654.
- (97) Geppert, J.; Röse, P.; Pauer, S.; Krewer, U. Microkinetic Barriers of the Oxygen Evolution on the Oxides of Iridium, Ruthenium and their Binary Mixtures. *ChemElectroChem* **2022**.
- (98) Geppert, J.; Kubannek, F.; Röse, P.; Krewer, U. Identifying the oxygen evolution mechanism by microkinetic modelling of cyclic voltammograms. *Electrochim. Acta* **2021**, *380*, 137902.
- (99) Wang, Y.; Laborda, E.; Ward, K. R.; Tschulik, K.; Compton, R. G. A kinetic study of oxygen reduction reaction and characterization on electrodeposited gold nanoparticles of diameter between 17 and 40 nm in 0.5 M sulfuric acid. *Nanoscale* **2013**, *5* (20), 9699–9708.
- (100) Marshall, A. T.; Herritsch, A. Understanding the Hydrogen and Oxygen Evolution Reactions through Microkinetic Models. *ECS Trans.* **2018**, *85* (11), 121.
- (101) Calderon-Cardenas, A.; Paredes-Salazar, E. A.; Mujica-Martinez, C. A.; Nagao, R.; Varela, H. Thorough Analysis of the Effect of Temperature on the Electro-Oxidation of Formic Acid. *J. Phys. Chem. C* **2020**, *124* (44), 24259–24270.
- (102) King, H. J.; Fournier, M.; Bonke, S. A.; Seeman, E.; Chatti, M.; Jumabekov, A. N.; Johannessen, B.; Kappen, P.; Simonov, A. N.; Hocking, R. K. Photon-Induced, Timescale, and Electrode Effects Critical for the in Situ X-ray Spectroscopic Analysis of Electrocatalysts: The Water Oxidation Case. *J. Phys. Chem. C* **2019**, *123* (47), 28533–28549.
- (103) Vodeb, O.; Lončar, A.; Bele, M.; Hrnjić, A.; Jovanović, P.; Gaberšek, M.; Hodnik, N. Intrinsic properties of nanoparticulate Ir-based catalysts for oxygen evolution reaction by AC voltammetry. *Electrochim. Acta* **2023**, *464*, 142882.
- (104) Snitkoff-Sol, R. Z.; Rimon, O.; Bond, A. M.; Elbaz, L. Direct measurement of the oxygen reduction reaction kinetics on iron phthalocyanine using advanced transient voltammetry. *Nature Catalysis* **2024**, *7* (2), 139–147.